A Single Envelope Modulator-Based Envelope-Tracking Structure for Multiple-Input and Multiple-Output Wireless Transmitters

Chao Yu, *Student Member*, *IEEE*, and Anding Zhu, *Member*, *IEEE*

***Abstract*—A single envelope modulator-based envelope tracking (ET) power amplifier (PA) structure with a related digital predistortion (DPD) technique for multiple-input and multiple-output (MIMO) wireless transmitters is presented in this paper. By generating a common tracking envelope, only one envelope modulator is employed for controlling supply voltage of the RF PAs in all branches in the system, which dramatically reduces the system implementation cost. Due to the structure change, additional distortion is introduced, and it is difficult to directly compensate by using the conventional DPD because the tracking envelope is no longer the same as the RF envelope and thus the MIMO ET PA becomes a two-input and one-output system. To resolve this problem, in this paper we propose a novel DPD technique in which the PA input and output data are reconstructed into multiple data subsets according to variations of the tracking envelope. It converts the 2-to-1 mapping into multiple 1-to-1 ones, where the conventional DPD can be employed again. Experimental results demonstrated that the distortion, including static nonlinearities, memory effects and additional distortion caused by the structure change, can be effectively compensated by using the proposed DPD technique. Compared to the conventional ET, the overall efficiency of the system is only slightly decreased, but the system cost is much lower because only one envelope modulator is required in the whole system.**

***Index Terms*—Digital predistortion, envelope tracking (ET), multiple-input and multiple-output (MIMO), power amplifier (PA), Volterra series.**

I. Introduction

DUE to the demands for large capacity and high performance, multiple-input and multiple-output (MIMO) technique plays an important role in modern wireless communication systems, such as IEEE 802.11n wireless LAN, Worldwide Interoperability for Microwave Access (WiMAX), and 3GPP Long Term Evolution (LTE) [1]. Orthogonal frequency division multiplexing (OFDM) is a popular modulation scheme, in which high-speed information data are divided into multiple lower-speed signals that are transmitted simultaneously on a large number of subcarriers that are orthogonal to each other. The OFDM combined with MIMO technology (MIMO-OFDM) is an attractive solution for future mobile communications due to its ability to support high data rates, large capacity, and robustness to multipath fading.

One of the main drawbacks of OFDM is that the transmit signal exhibits a high peak-to-average power ratio (PAPR), which often leads to very low efficiency of the RF power amplifier (PA) [2]. To resolve this problem, envelope tracking (ET) technique has been proposed to enable the RF PA to be operated continuously in the compression regime over a wide range of power levels by superimposing a control signal at the drain/collector of the RF amplifier according to the envelope variation of the transmit signal [3]. ET can significantly improve power efficiency of the system, especially for signals with a high PAPR. It is therefore desirable to employ the ET technique in the MIMO-OFDM system. However, the envelope modulator is often difficult to design and it may add to the system cost. If ET is used in each branch of the RF chain in MIMO, the system cost may be further increased in some circumstances.

To reduce cost, a MIMO ET structure employing one envelope modulator to control all RF branches of the MIMO transmitter can be used. It is achieved by inserting an envelope processing block in the envelope path that takes the envelope signals from all branches and generates a common envelope to be used as the common tracking signal for PAs in all RF branches. Since only one tracking envelope, that is, a common supply voltage, is used, additional distortion will be introduced to the system due to mis-synchronization between the supply voltage and the envelope of the RF transmit signal in each branch. This distortion is expected to be compensated by using digital predistortion (DPD).

In the past decade, many DPD models have been developed, but most of them are only suitable for a single input and single output system, such as memory polynomials [4], [5], augmented Wiener model [6], Hammerstein and Wiener models [7], and various truncated Volterra series [8]-[11]. In the MIMO ET system, because one common tracking signal is used to control all branches, the tracking signal is no longer the same as the envelope of the RF signal in each individual branch. Thus the PA becomes a two-input and one-output system, where the inverse function cannot be easily found, so that the conventional DPD can no longer be employed directly. In [12], a two-input and two-output model was proposed, but it can only be used for compensating distortion induced by cross-talks among the MIMO branches. In [13], a dual-input DPD model was proposed for linearizing PAs with dynamic load modulation and in [14][15], a similar approach was used for linearizing PAs with slow envelope tracking. These models

This work was supported by the Science Foundation Ireland under the Principal Investigator Award scheme.

The authors are with the School of Electrical, Electronic and Communications Engineering, University College Dublin, Dublin 4, Ireland (e-mail: chao.yu@ucdconnect.ie; anding.zhu@ucd.ie).

do not perform well in linearizing PAs in the MIMO ET system because these single function based models have limited capacity in capturing the large dynamic variations of PA characteristics under the high power MIMO conditions. These models also suffered from non-invertibility and high complexity problems. A lookup table-based memoryless predistortion was developed in [16] for compensating static nonlinearity and distortion induced by the bandwidth reduction of the envelope tracking signals in the ET system, but memory effects were not addressed.

In this paper, we propose a new predistortion methodology, in which we convert the 2-to-1 mapping into multiple 1-to-1 ones by dividing the transmit data stream into different data subsets, based on an assumption that the characteristics of the PA do not change with the supply voltage within a very small range. It allows the conventional single input and single output DPD models to be employed again. In order to compensate memory effects, neighboring samples are kept with the corresponding inputs together to build the inverse function for the DPD. Experimental results show that the proposed DPD technique not only effectively removes the distortion induced by the modification of the tracking signal, but also can compensate for standard nonlinearities in the ET system, such as memory effects induced by self-heating, trapping and matching networks. In addition, to ensure high efficiency and high linearity operation of the envelope modulator, effective signal smoothing and waveform shaping techniques are also proposed in this paper. Although more complex signal processing is required in the new system, the overall cost is greatly reduced because only one envelope modulator is employed in the whole MIMO system.

The paper is organized as follows. In Section II, a MIMO ET structure is introduced in comparison with the conventional ET. The envelope processing module for this ET structure is given in Section III. Section IV presents the new DPD technique, and the experimental results are given in Section V, with a conclusion in Section VI.

II. MIMO Envelope Tracking Structure

A. Conventional ET Structure

In an ET system, the drain (or collector) of the RF transistor in the RF power amplifier is dynamically controlled by the envelope modulator whose output is changing in proportion to the envelope magnitude of the RF input. This tracking process allows the RF PA to be continuously operated at near saturation region for a large range of signal levels, and therefore, high power efficiency can be obtained [3]. Although the output of the ET PA can be kept linear with the input over a wide range, there are inherent nonlinearities in the ET system [17]-[19]. Digital predistortion is thus normally employed to compensate for the nonlinearity in ET. Fig. 1 shows a conventional ET system structure, which consists of a signal source, a DPD unit, an envelope modulator, and an RF PA. A signal source generation module is used to generate digital baseband signals while the DPD creates the correction for the nonlinearity of the system. A high efficiency linear amplifier, called an envelope modulator, converts the RF envelope into a tracking waveform to supply the drain/collector voltage of the PA. Because the overall system can be treated as one box, the DPD unit is normally placed before the signal is split, and conventional DPD models can be employed [11].

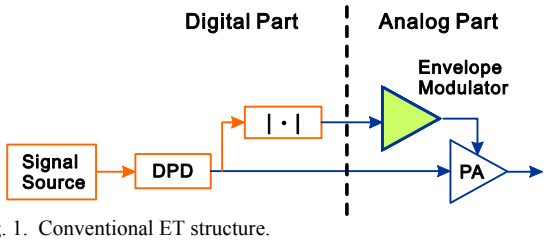

Fig. 1. Conventional ET structure.

The ET system shown in Fig. 1 can simultaneously provide high efficiency and high linearity. However, such systems cannot be directly employed in a MIMO transmitter. Since multiple RF chains, usually in a set of two or four, are employed in parallel in a MIMO system, multiple envelope tracking modules and DPD blocks must be used to control each RF PA and compensate for their nonlinearities, as shown in Fig. 2, where a 4×4 configuration of a MIMO system is taken as an example. This multiple-ET configuration significantly increases the cost of the transmitter.

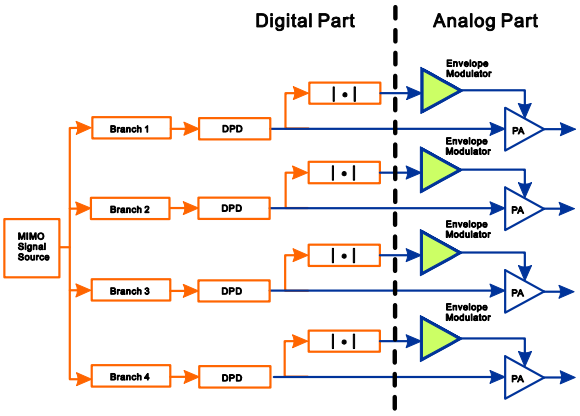

Fig. 2. Conventional ET structure for MIMO applications.

B. MIMO ET Structure

To reduce cost, one envelope modulator can be used to control all branches in the MIMO system, as shown in Fig. 3. In order to generate a common tracking envelope for all branches, one additional module, called *envelope processing*, is added to the structure. This block takes the envelope signals from all branches and generates a common envelope to be used as the common tracking signal for PAs in all RF branches. The modification, from generating its own envelope in each branch

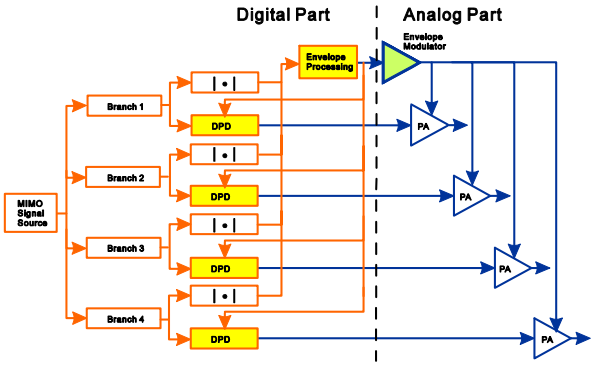

Fig. 3. Single modulator based MIMO ET structure.

alone to employing a common envelope for all branches, will introduce additional distortion that is expected to be compensated by the DPD module. Because the common envelope is shared, DPD modules for each branch, previously placed prior to the envelope generation module, now needs to be placed after the signal is split and in parallel with the envelope path.

Compared to the conventional ET, more signal processing operations must be conducted in the new structure, as we will introduce in the following sections. These algorithms can be implemented in digital circuits, which are generally cheap and thus they do not add much extra cost. However, removing multiple analog envelope modulators may appreciably reduce the overall system cost.

III. Common Tracking Signal Generation

In the MIMO ET structure, an additional signal processing operation must be conducted to generate the common envelope tracking signal from the multiple envelopes of the RF branches to control the multiple RF PAs since only one envelope modulator is employed in the whole system. Meanwhile, to ensure high efficiency and high linearity, certain requirements must be satisfied in generating the common control signal because each RF PA is still operated in the envelope tracking mode. In this section, we propose to generate the common tracking signal in three steps, as described below.

Step 1: Max Operation

In the ET operation, to avoid signal clipping, the drain supply voltage must be greater than the envelope magnitude of the RF signal to be transmitted, namely,

$$V_{DD}(t) \geq V_{env}(t) \tag{1}$$

where $V_{DD}(t)$ is the drain voltage and $V_{env}(t)$ is the envelope voltage of the RF input signal. To meet this requirement in all branches, one of the easiest ways of generating the common tracking signal is to conduct a maximum operation in the discrete time domain, that is,

$$\hat{e}(n) = \max\{e_1(n), ..., e_N(n)\} \tag{2}$$

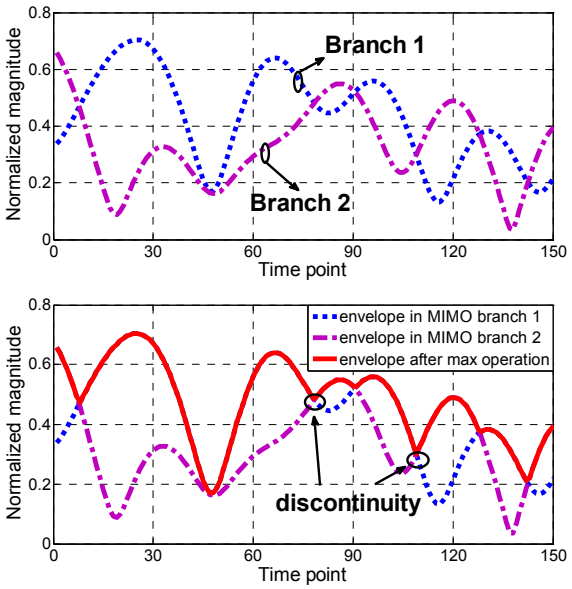

Fig. 4. Common envelope generation using maximum operation.

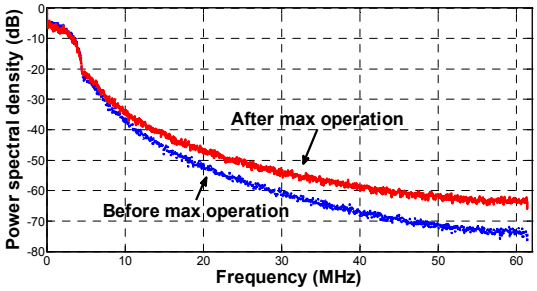

Fig. 5. The power spectral density of the envelope signal after maximum operation.

where $\hat{e}(n)$ is the normalized common envelope and $e_N(n)$ is the envelope of the N^{th} branch in the MIMO configuration. Let's take a 5 MHz LTE signal in 2×2 MIMO configuration as an example. As shown in Fig. 4, the common envelope is generated by taking the magnitude of two envelopes, whichever is higher at the sampling point.

Step 2: Smoothing Operation

Due to the max operation, the discontinuities in the common envelope will appear, as shown in Fig. 4. This will deteriorate the spectrum of the envelope since the high frequency components will significantly increase, as shown in Fig. 5. In a real system, the envelope modulator often has a limited operation bandwidth. If excited by a signal with a wider bandwidth, significant distortion will be introduced into the system. In order to amplify the envelope signal as linear as possible and simultaneously keep high efficiency, the common envelope after the max operation must be optimized. In the literature, several bandwidth reduction techniques have been proposed [16][20]. The techniques proposed in [16] are involving frequency domain filtering and time domain restoration, which is time consuming. The approach in [20] is not suitable for wideband signals.

In this paper, we propose a modified moving average method, which is fully operated in the discrete time domain and can be easily embedded in a digital circuit. It can be conducted in two steps. Firstly, we apply the general moving average to the common envelope in the discrete time domain. The general moving average method can effectively limit the bandwidth of the envelope signal, but the envelope cannot meet the requirement of (1), because some of the amplitudes of the new signal are below the original values, as shown in Fig. 6, which will cause signal clipping in the ET operation. To avoid this situation, in the second step, we restore the amplitudes that are below the existing values to the original ones to meet the requirement of (1). The operation is outlined as below:

(i) Moving Average:

$$\bar{e}(n) = \frac{1}{2k+1} \sum_{i=-k}^{k} \hat{e}(n+i) \tag{3}$$

(ii) Amplitude Restoration:

$$\begin{aligned} &If \ \ \bar{e}(n) < \hat{e}(n), \\ &then \ \ \bar{e}(n) = \hat{e}(n) \\ &else \ \ \bar{e}(n) = \bar{e}(n) \end{aligned} \tag{4}$$

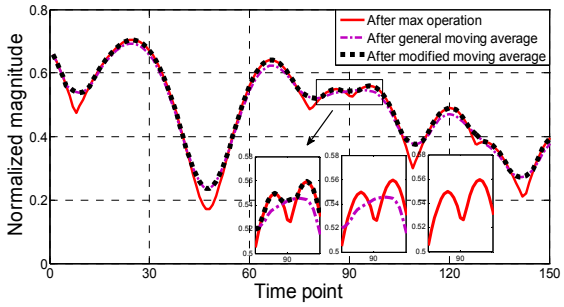

Fig. 6. The smoothing operation for the common envelope.

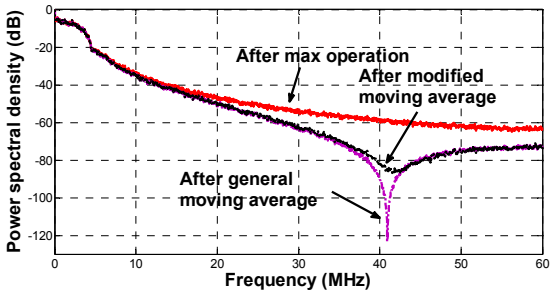

Fig. 7. The power spectral density of the envelope with smoothing operation of 3 points.

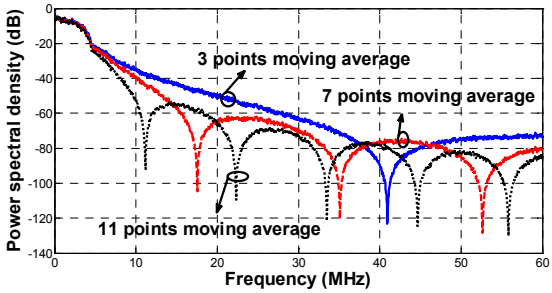

Fig. 8. The performance of general moving average using different number of data points.

where $\overline{e}(n)$ is the normalized envelope signal after smoothing operation. After this operation, not only the discontinuities in the envelope are removed and thus the bandwidth of the signal is effectively reduced, but also the modified envelope meets the requirement of (1), as shown in Figs. 6 and 7. Furthermore, steeper attenuation of the envelope spectrum can be obtained by increasing the number of moving average points in the time domain, which is shown in Fig. 8. Wide bandwidth optimization of the common envelope can also be realized by cascading several modified moving average modules with different numbers of moving average points, as shown in Fig. 9. For instance, after processed by three cascaded (11, 7, 3-points) modified moving average modules, the time domain waveform is effectively smoothed and the bandwidth of the signal is significantly reduced, shown in Figs. 10 and 11, respectively.

Step 3: Wave Shaping

Because the envelope modulator has a certain limit on the range of output voltages, the envelope signal needs to be mapped into the voltage range that the modulator can supply, by using a suitable wave shaping function before entering the modulator. In this paper, we employ the following shaping function to map the envelope amplitude to the supply voltage:

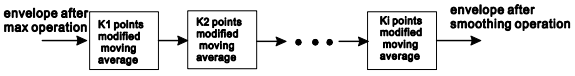

Fig. 9. The overall smoothing operation.

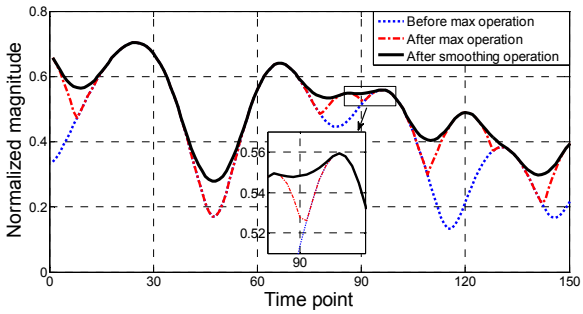

Fig. 10. Envelope after smoothing operation in the time domain.

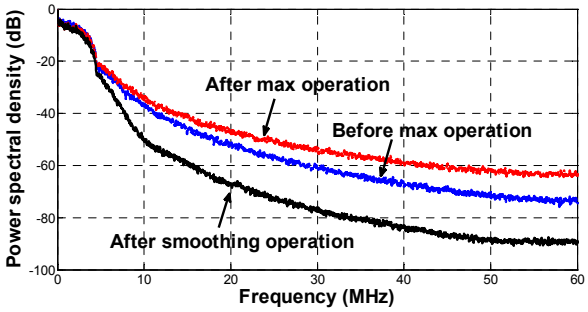

Fig. 11. Power spectral density of the envelope after smoothing operation.

$$V_{DD}(n) = \alpha V_{\min} + \beta (V_{\max} - V_{\min}) \times \overline{e}(n)^p \quad (5)$$

where V_{max} is the maximum shaped drain voltage, V_{min} is the minimum shaped drain voltage, α, β and p are constant factors. In this work, we choose α=1, β=1 and p=2. The $V_{DD}(n)$ is then normalized,

$$e(n) = V_{DD}(n) / \max(V_{DD}) \quad (6)$$

After these three steps above, a common envelope $e(n)$ is generated and is to be shared among all branches of the MIMO transmitter.

IV. Digital Predistortion

Due to the modification of the tracking envelope, additional distortion may be introduced. To correct these nonlinearities, digital predistortion must be employed. Because the tracking signal is no longer the same as the envelope of the RF signal, the conventional DPD is no longer applicable. In this section, we introduce a new DPD technique to linearize the MIMO ET system as described below.

A. 2-to-1 Mapping Problem

In the conventional ET, the envelope signal is generated directly from the RF input. The whole ET system can be treated as one box with a one-to-one mapping from input to output; the DPD thus can be placed before the signal split, as shown in Fig. 1. However, this is not the case that occurs in the MIMO ET. In the new structure, the envelope tracking signal is generated from multiple branches and then used for controlling supply voltages of all branches. In each individual branch, the tracking envelope is not identical as that generated from its RF

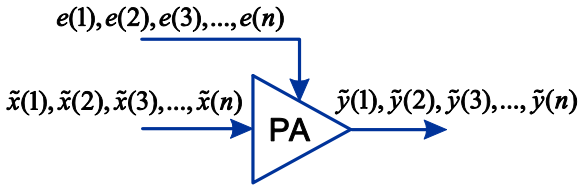

Fig. 12. Simplified ET structure.

signal any more, which means that for the same amplitude of the input $\tilde{x}(n)$, the supply voltage could be different, or vice versa, as shown in Fig. 12, where $e(n)$ does not necessarily equal to the envelope of $\tilde{x}(n)$. In a real system, since the gain of the PA normally varies with the supply voltage, it leads that the mapping from the input $\tilde{x}(n)$ to the output $\tilde{y}(n)$ can be different under different supply voltages, $e(n)$. The output of the PA, $\tilde{y}(n)$, now depends on not only the input $\tilde{x}(n)$, but also the tracking envelope signal, $e(n)$. In other words, the PA now becomes a 2-to-1 mapping system. The conventional 1-to-1 mapping is no longer applicable, and thus the conventional single input and single output DPD models cannot be directly employed in the new system any more.

B. Data Separation Procedure

In order to resolve this problem, in this paper we propose to convert the 2-to-1 mapping into multiple 1-to-1 ones by re-organizing the input and output data into different subgroups according to their corresponding common envelope values. For example, as shown in Fig. 13, $\tilde{x}(i)$, $\tilde{x}(j)$, $\tilde{x}(p)$, $\tilde{x}(q)$ are selected into the same group because their tracking envelope voltages are the same, i.e., they all are equal to E. The corresponding output samples $\tilde{y}(i), \tilde{y}(j), \tilde{y}(p), \tilde{y}(q)$ can also be selected. Following this procedure, specific input and output data sets can be obtained, as shown in Fig. 14.

If $E = e(i) = e(j) = e(p) = e(q) = \ldots$

then

$$X = [\tilde{x}(i) \quad \tilde{x}(j) \quad \tilde{x}(p) \quad \tilde{x}(q) \quad \ldots]$$
$$Y = [\tilde{y}(i) \quad \tilde{y}(j) \quad \tilde{y}(p) \quad \tilde{y}(q) \quad \ldots] \tag{7}$$

A single input and single output transfer function from $\tilde{x}(n)$ to $\tilde{y}(n)$ can then be constructed and an inverse function can be found because the characteristics of the PA are the same under the same tracking envelope. However, this idea cannot be directly implemented in a real world because an infinite number of transfer functions will be needed if every common envelope value is used.

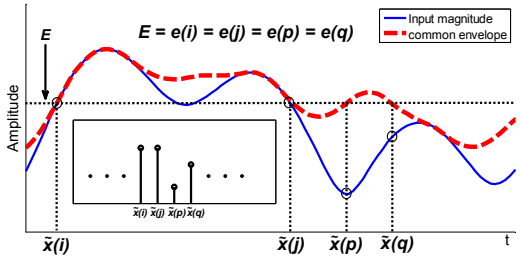

Fig. 13. Data separation procedure.

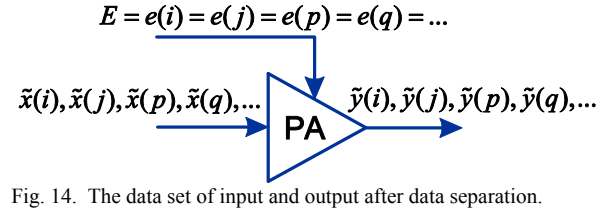

Fig. 14. The data set of input and output after data separation.

Fortunately, in practice, although the characteristic of the PA often changes with its supply voltage, the variation is very small if the voltage fluctuation is in a small range. This means that the same function can be used to represent the PA behavior within a small change of the supply voltage. In other words, we can select the data samples according to a range of values of *e*(n) rather than a single value. To proceed, we define a set of thresholds

$$\tau = \{\lambda_1, \lambda_2, \ldots, \lambda_S\} (\lambda_1 < \lambda_2 < \ldots < \lambda_S) \tag{8}$$

where λ_i is the i^{th} threshold and S is the total number of thresholds. We also set $\lambda_0 = 0$ and $\lambda_{S+1} = 1$. By using these thresholds, the common envelope tracking signal $e(n)$ can be divided into S+1 intervals:

$$E_k = (\lambda_{k-1} \quad \lambda_k], 1 \le k \le S+1 \tag{9}$$

The input and output data can then be separated into S+1 data subsets according to these intervals:

$$If \quad e(n) \in E_k$$
$$then \quad \tilde{x}(n) \in X_k, \tilde{y}(n) \in Y_k \tag{10}$$

where E_k is the k^{th} interval of envelope signal, X_k is the k^{th} data subset of input signal, and Y_k is the k^{th} data subset of output signal.

In a wideband system, memory effects appear significantly, which lead that the output of the PA depends on not only the instantaneous input but also the past of the input. To compensate for memory effects, the previous samples of the input must be built into the nonlinear function of the DPD. The data selection process above only considers the instantaneous relationships between the input and the output and cannot be directly used to build the transfer function of a memory DPD because the memory samples may fall in a different subset of the data. To resolve this problem, we propose to keep a few neighboring points as memory samples when forming the data subsets. For example, in Fig. 15, $\tilde{x}(q-1)$ is kept and treated as the 1st memory point of $\tilde{x}(q)$. The same procedure will be applied to other sampling points. The data separation process (10) is modified as below:

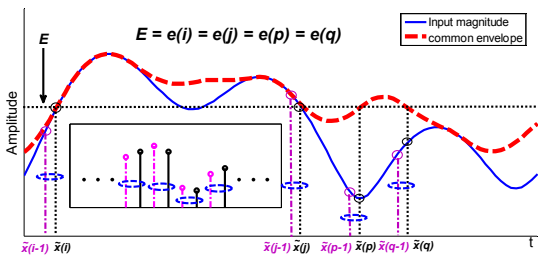

Fig. 15. Data separation procedure for memory DPD.

$$\begin{aligned} &If \quad e(n) \in E_k \\ &then \\ &\quad \tilde{x}(n) \in X_k, \tilde{x}(n-1) \in X_k, \cdots, \tilde{x}(n-M) \in X_k, \\ &\quad \tilde{y}(n) \in Y_k, \tilde{y}(n-1) \in Y_k, \cdots, \tilde{y}(n-M) \in Y_k \end{aligned} \tag{11}$$

where M represents memory length and normally has a small value, such as M=1, 2, 3. The final divided data subset can be represented by

$$D_k = [X_k \quad Y_k], 1 \le k \le S+1 \tag{12}$$

where D_k is the k^{th} data subset.

C. DPD Model Selection and System Structure

In the original MIMO ET system, the output of the PA depends on not only its RF input but also its tracking envelope. After data separation, the 2-to-1 mapping is now converted to multiple 1-to-1 ones. For instance, for each subset of input and output data, which are gathered according to the corresponding tracking signal values, the output now depends on the input only. In this case, conventional DPD models can be employed again.

In this work, the low-pass equivalent format of the first-order dynamic deviation reduction-based Volterra series [21] is chosen as the DPD function for each data subset. Indirect learning can be utilized for the model parameter extraction, where the output of the PA $\tilde{y}(n)$ is used as the input while the input of the PA $\tilde{x}(n)$ is as the expected output. For example, for the k^{th} data subset $D_k = [X_k \quad Y_k]$, its DPD function can be written as

$$\begin{aligned} \tilde{x}_k(n) &= G_k[\tilde{y}_k(n)] \\ &= \sum_{p=0}^{\frac{P-1}{2}} \sum_{i=0}^{M} \tilde{g}_{k,2p+1,1}(i) \left|\tilde{y}_k(n)\right|^{2p} \tilde{y}_k(n-i) \\ &\quad + \sum_{p=1}^{\frac{P-1}{2}} \sum_{i=1}^{M} \tilde{g}_{k,2p+1,2}(i) \left|\tilde{y}_k(n)\right|^{2(p-1)} \tilde{y}_k{}^2(n) \tilde{y}_k{}^*(n-i) \end{aligned} \tag{13}$$

where $\tilde{g}_{k,2p+1,j}(\cdot)$ (j=1,2) is the k^{th} data subset of complex Volterra kernel. P is an odd number representing the order of the nonlinearity while M represents the memory length. Since the output is linear with respect to the coefficients, Least Squares (LS) algorithm can be employed to extract the DPD coefficients. In a matrix form, the LS-based model extraction operation [22] can be represented as

$$C_{L\times 1} = [Y^H{}_{L\times N} Y_{N\times L}]^{-1} Y^H{}_{L\times N} X_{N\times 1} \tag{14}$$

where $X_{N\times 1}$ and $Y_{N\times L}$ are the input and output matrix formed from (13) for N data samples. $C_{L\times 1}$ is the coefficients matrix and L is the number of coefficients. $(\cdot)^H$ represents the Hermitian transpose and $[\cdot]^{-1}$ represents matrix inverse. According to (12), there are S+1sets of DPD parameters to be extracted.

Once the coefficients are extracted, the new MIMO ET system with digital predistortion can be constructed as illustrated in Fig. 16. The common tracking envelope $e(n)$ is generated from the envelope signals $e_1(n)$, $e_2(n)$,…, $e_N(n)$ of multiple branches and then used as the input to the common envelope modulator. In each branch, the DPD function is represented by,

$$\begin{aligned} \tilde{u}(n) &= \sum_{p=0}^{\frac{P-1}{2}} \sum_{i=0}^{M} \tilde{g}_{k(e(n)),2p+1,1}(i) \left|\tilde{x}(n)\right|^{2p} \tilde{x}(n-i) \\ &\quad + \sum_{p=1}^{\frac{P-1}{2}} \sum_{i=1}^{M} \tilde{g}_{k(e(n)),2p+1,2}(i) \left|\tilde{x}(n)\right|^{2(p-1)} \tilde{x}^2(n) \tilde{x}^*(n-i) \end{aligned} \tag{15}$$

where $\tilde{x}(n)$ and $\tilde{u}(n)$ are the original input and the predistorted output, respectively. $\tilde{g}_{k(e(n)),2p+1,j}(\cdot)$ is the coefficient, whose value is selected from the coefficient subsets controlled by the corresponding value of the tracking envelope $e(n)$. For instance, if $e(n) \in E_k$, $\tilde{g}_{k,2p+1,j}(\cdot)$ is chosen as the present set of DPD coefficients.

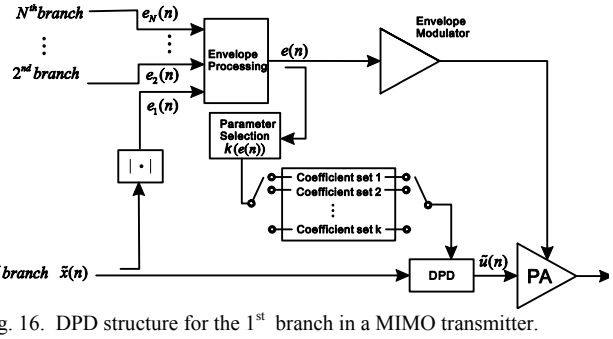

Fig. 16. DPD structure for the 1st branch in a MIMO transmitter.

D. System Complexity Analysis

Compared to conventional single input and single output DPDs, more digital signal processing (DSP) is required in the proposed approach, but these DSP is mainly conducted in the model extraction process. In the implementation of the DPD unit itself, there is only one equation required, which is the same as the conventional DPDs. The only difference is that, instead of using the same coefficients for all the input samples, we select the coefficients for each input sample in the RF chain according to its corresponding instantaneous value of the tracking envelope. It requires small memory logic to store the pre-extracted multiple sets of coefficients and a control circuit for coefficients selection. This implementation is straightforward, and it is very simple and with low cost.

Compared to the dual-input model [13], the complexity of the proposed approach is actually much lower. Since the tracking signal is no longer the same as the envelope of the RF input, complex nonlinearities occur in the MIMO-ET system. It is very difficult to describe these nonlinearities by using a single function. If the dual-input model is employed, a large number (typically two or three hundred) of coefficients are required. It dramatically increases the model extraction complexity and system implementation cost. For instance, if 2,000 samples are used for model extraction with 300 coefficients, 387,600,000 multiplication operations are required in solving the LS matrix [22]. In our approach, the effects of the supply voltage are separated from the distortion caused by the normal nonlinearity of the PA. For each given supply voltage, the PA is operated similar to a normal class-AB mode. This PA behavior can be accurately described by using a very simple function, e.g., a 1st-order truncated DDR-Volterra model with a small number (typically less than thirty) of coefficients. Therefore, even if we need to extract multiple sets

TABLE I
DPD PERFORMANCE OF PROPOSED MODEL AND DUAL-INPUT MODEL

	Number of Coefficients	Pout (dBm)	Efficiency* (%)	NRMSE (%)	ACLR(-/+5MHz) (dBc)	ACLR(-/+10MHz) (dBc)
Without DPD	N/A	46.11	44.27	15.96	-23.83/-23.25	-37.60/-37.00
Dual-input Model [13]	300	44.99	40.51	1.64	-47.61/-47.93	-52.09/-51.31
Proposed Model	17 (100 sets)	44.95	40.53	1.07	-52.88/-53.64	-55.80/-55.18

* Efficiency here is overall efficiency, including the envelope modulator and the PA.

of coefficients, the system complexity is still very low compared to the dual-input model. For example, for the same 2,000 samples, only 119,491,300 multiplication operations [22] are needed in our approach in the model extraction with 17 coefficients, even if we repeat 100 times to extract 100 sets of coefficients. Furthermore, the multiple model extraction process can be conducted repeatedly by using the same LS blocks because all the models have identical structures. In the real implementation, we only need to implement one set of LS operation units and reuse them in the signal process, which significantly reduces implementation cost.

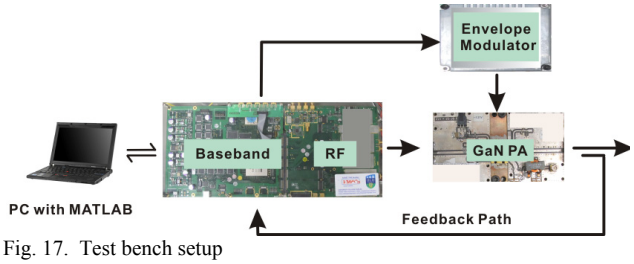

Fig. 17. Test bench setup

V. EXPERIMENTAL RESULTS

The MIMO ET structure with the proposed DPD algorithm was verified by experimental measurements. The test bench set up is shown in Fig. 17, which includes a PC with Matlab software, a baseband and an RF board, a high power GaN PA, and an envelope modulator. The main PA was operated at 2.14 GHz and was biased at Class-AB mode with V_{GS} =-1.21V. The drain voltage V_{DD} was controlled by the envelope modulator. The tracking voltage was varied from 25 to 60V. Standard 5 and 20 MHz LTE signals with 6.5dB PAPR in 2×2 and 4×4 MIMO configurations were used for the tests. The average output power of the PA was 45dBm.

A. Proposed Approach vs. State of the Art

In order to compare the performance with the state of the art, we implemented several relevant approaches and models published in the literature [13]-[15] on our test bench. The best performance we could obtain among these models was achieved by the dual-input model [13], as presented here.

The dual-input model was proposed for linearizing power amplifiers with varactor-based dynamic load modulation, and it was only tested with a low power PA excited with a 5 MHz signal. In this test, a high power PA with envelope tracking was employed, and a 5 MHz LTE signal with 6.5dB PAPR in 2×2 MIMO configuration was used. The exactly same system configuration was applied for both the approach in [13] and the proposed approach. The common tracking envelope was generated from two branches of the MIMO transmit chain, and then used for controlling the supply voltage of the PA at one branch. With the proposed approach, the input and output samples were re-grouped into 100 subsets and a 1st-order truncated DDR-Volterra model was employed with the nonlinear order P=11 and memory length M=1, and 17 coefficients in total. With the dual-input model, in order to find the optimum coefficients, we conducted an exhausted search by sweeping the parameters in Equation (10) in [13]. The best performance was achieved by selecting N_1=N_2=N_3=10, M_1=M_2=M_3=1, L_1=L_2=1, M_v=1, P=2, and 300 coefficients in total. The normalized root mean square error (NRMSE) and adjacent channel leakage ratio (ACLR) are given in Table I, and the frequency spectra are plotted in Fig. 18, where we can see that the proposed approach is at least 5 dB better in ACLR than the dual-input model for this particular test. For signals with wider bandwidths, the performance of the dual-input model was much worse. As discussed in Section IV.D, in terms of system implementation, the dual-input model is much more complex than the proposed approach because a very large number of coefficients are involved.

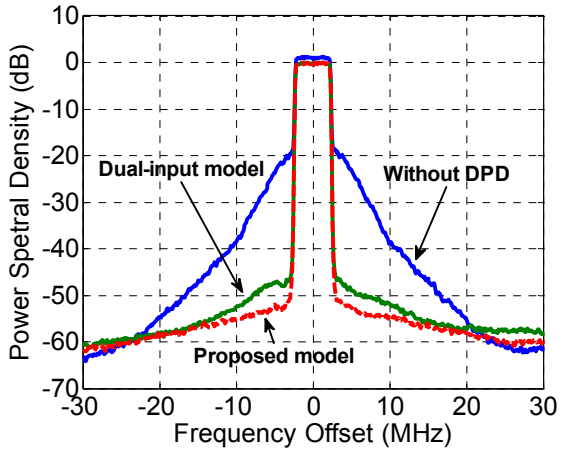

Fig. 18. Measured power spectral density with and without DPD.

B. Conventional ET vs. MIMO ET

In the ET, the power efficiency improvement is achieved by dynamically varying the drain supply voltage of the RF PA according to the envelope variations of the input signal. In principle, the best power efficiency is obtained when the best tracking accuracy is operated. In the MIMO ET, the tracking voltage is no longer accurately following the RF envelope due to the common tracking operation. The first question to ask is: how much efficiency degradation will be suffered in the new system. To answer this question, we

TABLE II
PERFORMANCE OF MIMO ET VS. CONVENTIONAL ET STRUCTURES

		Pout (dBm)	Efficiency* (%)	NRMSE (%)	ACLR(-/+20MHz) (dBc)	ACLR(-/+40MHz) (dBc)
One MIMO Branch	Conventional ET	45.58	45.32	5.17	-33.62/-32.31	-40.86/-41.04
	MIMO ET (2X2)	46.08	43.65	14.54	-26.34/-24.07	-40.08/-37.61
	MIMO ET (4X4)	46.40	42.34	16.92	-24.65/-22.82	-40.10/-37.34

* Efficiency here is overall efficiency, including the envelope modulator and PA.

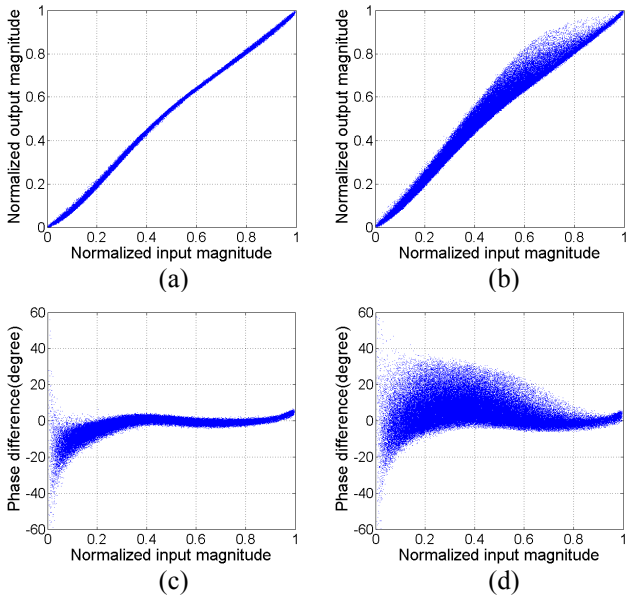

Fig. 19. AM-AM characteristics: (a) conventional ET (b) MIMO ET; AM-PM characteristics: (c) conventional ET (d) MIMO ET.

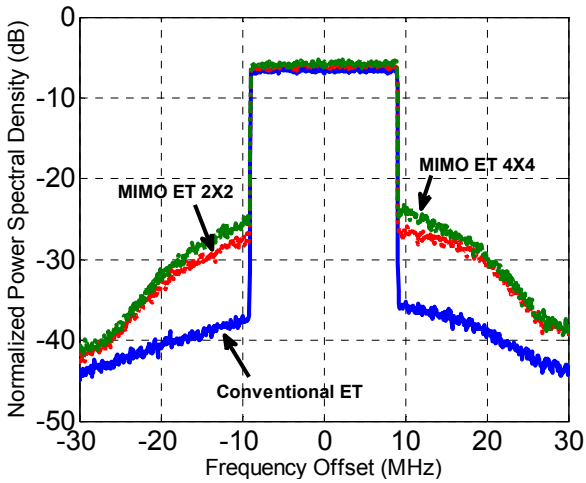

Fig. 20. Measured power spectral density in conventional ET and MIMO ET.

conducted three tests by operating the same PA with a 20 MHz LTE signal in three different modes: (i) in the conventional ET mode, where the tracking signal was directly generated from its RF input; (ii) in 2 x 2 MIMO mode, where the tracking envelope was generated from two inputs; and (iii) in 4 x 4 MIMO mode, where the tracking envelope was generated from four inputs. The results are listed in TABLE II, where we can see that, for almost the same output power, the efficiency degradation is very small, e.g., less that 3%, from one branch to four.

The results seem surprising, but they are actually true and reasonable, especially for wideband signals. That is because the overall efficiency of the ET is affected by the efficiencies of both the RF PA and the modulator. In fact, accurate tracking could achieve the best efficiency of the RF PA. However, accurate tracking may require the modulator to handle a very wideband envelope signal. Due to physical limits of the existing device technologies, the efficiency of the modulator may decrease quickly when the bandwidth of the excitation signal increases, because switching loss is significantly increased in the modulator. Therefore, the overall efficiency is often compromised by signal bandwidth and tracking accuracy. In the MIMO ET, the efficiency of the RF PA is slightly reduced, but the efficiency of the modulator is still maintained or even increased by employing a properly designed envelope tracking signal. The overall efficiency of the system thus does not decrease significantly.

However, the linearity of the system will deteriorate, as shown in the AM/AM and AM/PM plots in Fig. 19. In the conventional ET, the system can be kept fairly linear although some inherent nonlinearity exists. However, in the MIMO ET mode, significant distortion is introduced due to modification of the tracking signal. It is because the gain of the PA often varies with its supply voltage, distortion will occur if the tracking signal is not synchronized with the RF envelope. This phenomenon also can be observed from the frequency domain spectra plots in Fig. 20, where we can see that the out of band distortion is much higher in the MIMO system, and it becomes worse when more branches are employed. The values of NRMSE and ACLR are also presented in TABLE II.

C. DPD Performance

In order to evaluate linearization performance, two types of DPD were employed: (i) Memoryless DPD, where the memory length was set to zero; (ii) Memory DPD, where the memory length was set to 1. A 20MHz LTE signal is used as the test signal with 2×2 MIMO and 4×4 MIMO configurations. Fig. 21 shows AM/AM and AM/PM characteristics of the PA in one of the branches in the 2×2 MIMO configuration. Before DPD, we can see that significant distortion occurs. With the memoryless DPD, the majority distortion is removed, leaving only small residuals. While with the memory DPD, the nonlinearity is almost completely compensated, including the additional distortion and inherent nonlinearity in the ET. Fig. 22 shows the measured power spectral density of the output signal, where we can see that the out of band distortion is dramatically reduced with the memoryless DPD and a further improvement can be made with the memory DPD. Similar performance was achieved in the other branch in the 2×2 MIMO configuration.

Table III gives a summary of the system performance for

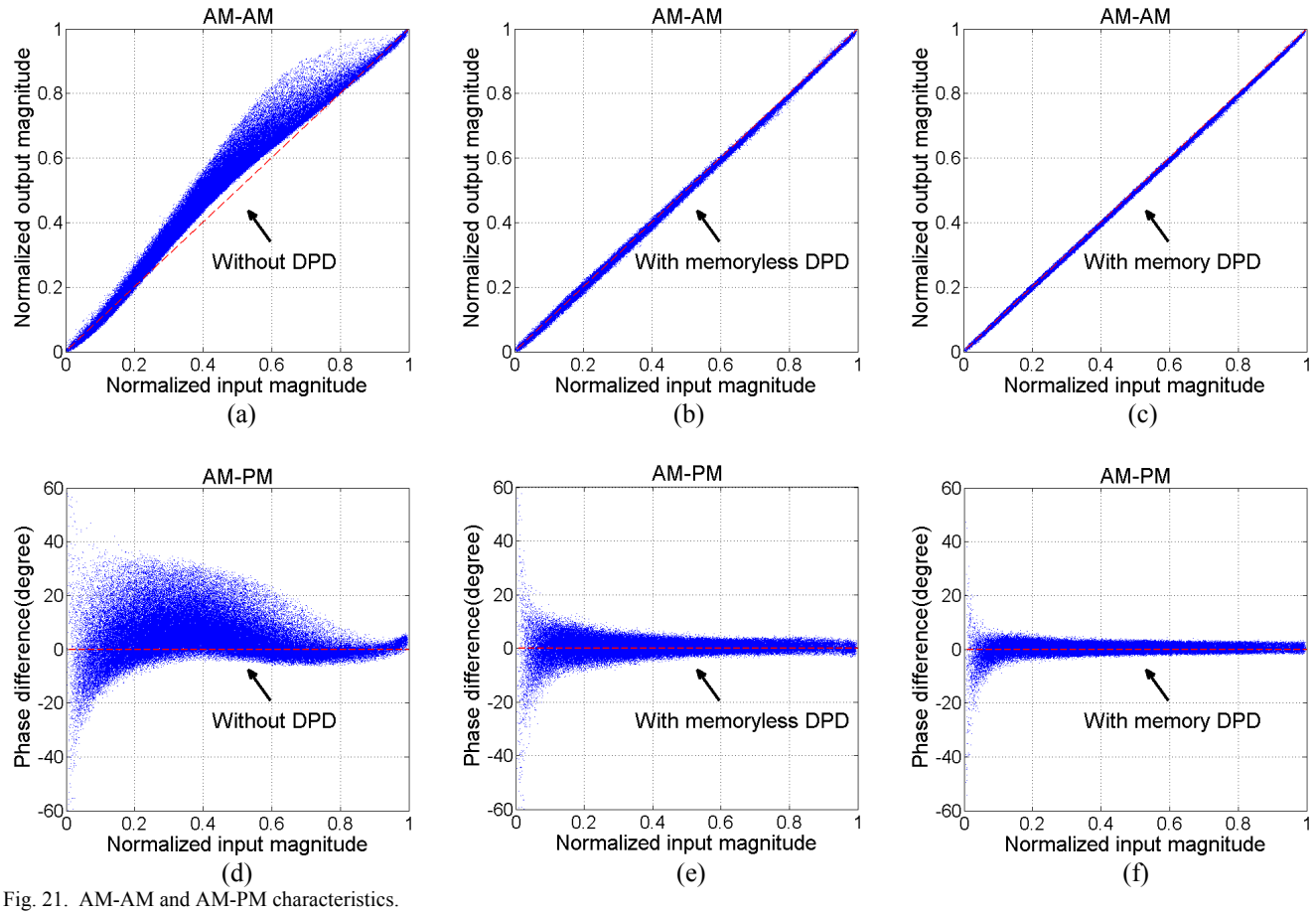

Fig. 21. AM-AM and AM-PM characteristics.

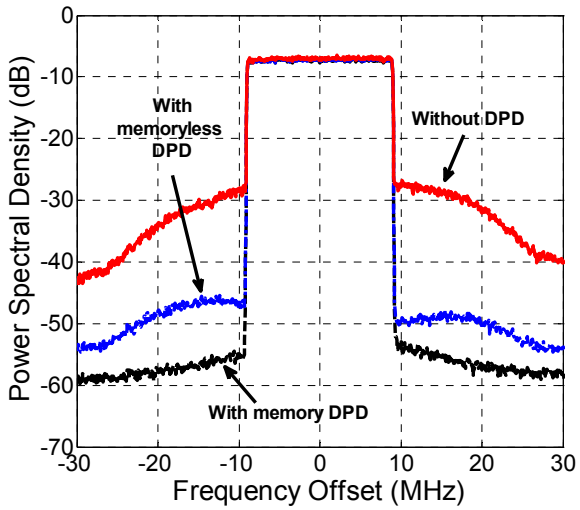

Fig. 22. Measured power spectral density of the output signal.

both branches in the 2×2 MIMO configuration. For branch 1, the NRMSE is improved from 14.4% to 3.22% with a memoryless DPD and further improved to 2.17% with a memory DPD. The ACLRs are as low as -43 and -49dBc at 20 and 40 MHz offsets with a memoryless DPD, and -50 and -51 dBc with a memory DPD, respectively. The efficiency is dropped by 2% due to the DPD operation. For branch 2, the ACLRs are also as low as -43 and -49 dBc at 20 and 40 MHz offsets with a memoryless DPD, and -50 and -52 dBc with a memory DPD, respectively. The efficiency is dropped by 3% due to the DPD operation.

The measured performance in 4×4 MIMO configuration is summarized in Table IV. Due to the common envelope is generated by envelope signals from four branches, the ACLRs performance before DPD is worse than that in the 2×2 MIMO configuration, e.g., further 2 dB deterioration, from -26 dBc to -24 dBc at 20 MHz offset. After memory DPD linearization, the ACLRs performance is improved by 24 dB, reaching -48 and

TABLE III
SYSTEM PERFORMANCE WITH AND WITHOUT DPD IN 2×2 MIMO CONFIGURATION

		Pout (dBm)	Efficiency* (%)	NRMSE (dB)	ACLR(-/+20MHz) (dBc)	ACLR(-/+40MHz) (dBc)
MIMO Branch 1	Without DPD	46.09	43.4	14.4	-26.08/-24.00	-39.73/-37.42
	Memoryless DPD	45.17	40.67	3.22	-43.54/-41.18	-49.23/-48.45
	Memory DPD	45.16	41.1	2.17	-50.58/-50.10	-51.71/-51.35
MIMO Branch 2	Without DPD	46.08	43.65	14.54	-26.34/-24.07	-40.08/-37.61
	Memoryless DPD	45.11	40.49	2.75	-41.43/-43.32	-49.26/-48.93
	Memory DPD	45.07	40.26	1.96	-50.38/-50.08	-52.00/-51.13

* Efficiency here is overall efficiency, including the envelope modulator and PA.

TABLE IV
SYSTEM PERFORMANCE WITH AND WITHOUT DPD IN 4×4 MIMO CONFIGURATION

		Pout (dBm)	Efficiency (%)	NRMSE (%)	ACLR(-/+20MHz) (dBc)	ACLR(-/+40MHz) (dBc)
MIMO Branch 1	Without DPD	46.38	42.14	16.57	-24.91/-23.09	-40.11/-37.67
	Memoryless DPD	45.17	37.86	3.36	-44.02/-41.58	-49.61/-48.96
	Memory DPD	45.15	37.68	2.64	-48.21/-48.12	-50.51/-49.37
MIMO Branch 2	Without DPD	46.40	42.14	16.85	-24.64/-22.79	-40.15/-37.31
	Memoryless DPD	45.09	37.17	2.91	-41.21/-40.99	-47.30/-43.95
	Memory DPD	45.17	37.98	2.79	-48.38/-47.03	-50.84/-49.78
MIMO Branch 3	Without DPD	46.40	42.34	16.92	-24.65/-22.82	-40.10/-37.34
	Memoryless DPD	45.23	37.84	2.84	-43.07/-40.37	-48.08/-46.09
	Memory DPD	45.18	37.94	1.76	-49.01/-47.73	-50.97/-50.63
MIMO Branch 4	Without DPD	46.45	42.63	16.66	-24.77/-22.82	-40.17/-37.39
	Memoryless DPD	45.18	37.74	3.53	-43.13/-41.18	-49.18/-47.15
	Memory DPD	45.17	37.98	1.95	-48.91/-48.00	-50.77/-50.54

* Efficiency here is overall efficiency, including the envelope modulator and PA.

-50 dBc at 20 and 40 MHz offset for all branches. Compared to the one in 2×2 MIMO configuration, the efficiency for each branch is dropped by 3%, from 40% to 37%. The AM/AM, AM/PM, and spectra performance are very similar to those shown in Figs. 21 and 22. To avoid duplication, we do not include them here.

VI. CONCLUSION

In this paper, an ET structure for MIMO applications is presented, where only one envelope modulator is employed, which significantly reduces the cost of the system. It is achieved by inserting an envelope processing block in the envelope path that takes the envelope signals from all branches and generates a common envelope to be used as the common tracking signal for PAs in all RF branches. Because only one common supply voltage is used, the tracking envelope is no longer synchronized with the RF envelope and thus additional distortion is introduced to the system due to the gain variations of the RF PA in each branch. To compensate this distortion, we proposed a new digital predistortion technique, where the 2-to-1 mapping is converted into multiple 1-to-1 ones and thus conventional DPDs can be employed in each data subset. Experimental results have demonstrated that, the nonlinear distortion in the system can be effectively compensated by the proposed DPD. Although the power efficiency is slightly dropped due to the structure change, the cost of the overall system is dramatically reduced since only one envelope modulator is employed. As price pressure becomes more demanding in the commercial market, the proposed solution will be very attractive in the future MIMO transmitter development.

ACKNOWLEDGEMENT

The authors would like to thank Gerard Wimpenny of Nujira Ltd. for proposing the MIMO ET structure described in Section II.

REFERENCES

[1] M. Rumney, *LTE and the Evolution to 4G Wireless: Design and Measurement Challenges*. Agilent Technologies, 2009

[2] S. C. Cripps, *RF Power Amplifiers for Wireless Communications*, 2nd ed. Norwood, MA: Artech House, 2006.

[3] F. H. Raab, P. Asbeck, S. Cripps, P. B. Kenington, Z. B. Popović, N. Pothecary, J. F. Sevic, and N. O. Sokal, "Power amplifiers and transmitters for RF and microwave," *IEEE Trans. Microw. Theory Tech.*, vol. 50, no. 3, pp. 814–826, Mar. 2002.

[4] J. Kim and K. Konstantinou, "Digital predistortion of wideband signals based on power amplifier model with memory," *Electron. Lett.*, vol. 37, no. 23, pp. 1417–1418, Nov. 2001.

[5] L. Ding, G. T. Zhou, D. R. Morgan, Z. Ma, J. S. Kenney, J. Kim, and C. R. Giardina, "A robust digital baseband predistorter constructed using memory polynomials," *IEEE Trans. Commun.*, vol. 52, no. 1, pp. 159–165, Jan. 2004.

[6] T. Liu, S. Boumaiza, and F. M. Ghannouchi, "Pre-compensation for the dynamic nonlinearity of wideband wireless transmitters using augmented Wiener predistorters," in *Proc. Asia–Pacific Microw. Conf.*, Suzhou, China, Dec. 2005, vol. 5, pp. 4–7.

[7] V. J. Mathews and G. L. Sicuranza, *Polynomial Signal Processing*. New York: Wiley, 2000.

[8] G. Montoro, P. L. Gilabert, E. Bertran, A. Cesari, and D. D. Silveira, "A new digital predictive predistorter for behavioral power amplifier linearization," *IEEE Microw. Wireless Compon. Lett.*, vol. 17, no. 6, pp. 448–450, Jun. 2007.

[9] C. Eun and E. J. Powers, "A new Volterra predistorter based on the indirect learning architecture," *IEEE Trans. Signal Process.*, vol. 45, no. 1, pp. 223–227, Jan. 1997.

[10] A. Zhu and T. J. Brazil, "An adaptive Volterra predistorter for the linearization of RF high power amplifiers," in *IEEE MTT-S Int. Microw. Symp. Dig.*, May 2002, pp. 461–464.

[11] A. Zhu , P. J. Draxler , H. Chin , T. J. Brazil , D. F. Kimball and P. M. Asbeck, "Digital predistortion for envelope-tracking power amplifiers using decomposed piecewise Volterra series", *IEEE Trans. Microw. Theory Tech.*, vol. 56, no. 10, pp. 2237-2247 , Oct. 2008.

[12] S. A. Bassam, W. Chen, M. Helaoui, F. M. Ghannouchi, Z. Feng, "Linearization of concurrent dual-band power amplifier based on 2D-DPD technique," *IEEE Microw. Wireless Compon. Lett.*, vol. 21, no. 12, pp. 685-687, Dec. 2011.

[13] H. Cao, H. M. Nemati, A. S. Tehrani, T. Eriksson, C. Fager, "Digital predistortion for high efficiency power amplifier architectures using a dual-input modeling approach," *IEEE Trans. Microw. Theory Tech.*, vol. 60, no. 2, pp. 361-369, Feb. 2012.

[14] P. L. Gilabert, G. Montoro, "Look-up table implementation of a slow envelope dependent digital predistorter for envelope tracking power amplifiers," *IEEE Microw. Wireless Compon. Lett.*, vol. 22, no. 2, pp. 97-99, Feb. 2012.

[15] G. Montoro, P. L. Gilabert, J. Berenguer, E. Bertran, "Digital predistortion of envelope tracking amplifiers driven by slew-rate limited envelopes," in *IEEE MTT-S Int. Microw. Symp. Dig.*, Jun. 2011, pp. 1–4.

[16] J. Jeong, D. F. Kimball, M. Kwak, C. Hsia, P. Draxler, and P. M. Asbeck, "Wideband envelope tracking power amplifiers with reduced bandwidth power supply waveforms and adaptive digital predistortion techniques," *IEEE Trans. Microw. Theory Tech.*, vol. 57, no. 12, pp. 3307–3314, Dec. 2009.

[17] D. F. Kimball, J. Jeong, C. Hsia, P. Draxler, S. Lanfranco, W. Nagy, K. Linthicum, L. E. Larson, and P. M. Asbeck, "High-efficiency envelope-tracking W-CDMA base-Station amplifier using GaN HFETs," *IEEE Trans. Microw. Theory Tech.*, vol. 54, no. 11, pp. 3848–3856, Nov. 2006.

[18] F. Wang, A. H. Yang, D. F. Kimball, L. E. Larson, and P. M. Asbeck, "Design of wide-bandwidth envelope-tracking power amplifiers for

OFDM applications," *IEEE Trans. Microw. Theory Tech.*, vol. 53, no. 4, pp. 1244–1255, Apr. 2005.

[19] F. Wang, D. F. Kimball, D. Y. Lie, P. M. Asbeck, and L. E. Larson, "A monolithic high-efficiency 2.4-GHz 20-dBm SiGe BiCMOS envelope-tracking OFDM power amplifier," *IEEE J. Solid-State Circuits*, vol. 42, no. 6, pp. 1271–1281, Jun. 2007.

[20] A. Cesari, A. Cid-Pastor, C. Alonso, J. M. Dilhac, "A DSP structure authorizing reduced-bandwidth DC/DC converters for dynamic supply of RF power amplifiers in wideband applications," *IEEE Industrial Electronics, IECON 2006 - 32nd Annual Conference on* , Nov. 2006, pp.3361-3366.

[21] A. Zhu, P. J. Draxler, J. J. Yan, T. J. Brazil, D. F. Kimball, and P. M. Asbeck, "Open-loop digital predistorter for RF power amplifiers using dynamic deviation reduction-based Volterra series," *IEEE Trans. Microw. Theory Tech.*, vol. 56, no. 7, pp. 1524–1534, Jul. 2008.

[22] L. Guan, and A. Zhu, "Optimized low-complexity implementation of least squares based model extraction for digital predistortion of RF power amplifiers", *IEEE Trans. Microw. Theory Tech.*, vol.60, no.3, pp.594-603, Mar. 2012.

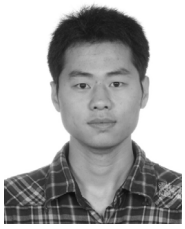

Chao Yu (S'09) received the B.E. and M.E. degree from School of Information Science and Engineering, Southeast University, Nanjing, China, in 2007 and 2010, respectively. He is currently working toward the Ph.D. degree at University College Dublin, Dublin, Ireland.

His research interests include antenna design, behavioral modeling and digital predistortion for RF power amplifiers.

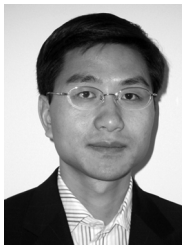

Anding Zhu (S'00-M'04) received the B.E. degree in telecommunication engineering from NorthChina ElectricPower University, Baoding, China, in 1997, and the M.E. degree in computer applications from Beijing University of Posts and Telecommunications, Beijing, China, in 2000, and the Ph.D. degree in electronic engineering from University College Dublin (UCD), Dublin, Ireland, in 2004.

He is currently a Lecturer with the School of Electrical, Electronic and Communications Engineering, UCD. His research interests include high-frequency nonlinear system modeling and device characterization techniques with a particular emphasis on Volterra-series-based behavioral modeling and linearization for RF PAs. He is also interested in wireless and RF system design, digital signal processing and nonlinear system identification algorithms.